

# MMT and Magellan infrared spectrograph

B. McLeod, G. Nystrom, H. Bergner, W. Brown, M. Burke, D. Curley, D. Fabricant, G. Furesz, J. Geary, E. Hertz, K. McCracken, T. Norton

Harvard-Smithsonian Center for Astrophysics, 60 Garden St., Cambridge MA, 02138 USA

## ABSTRACT

The MMT and Magellan infrared spectrograph (MMIRS) is a cryogenic multislit spectrograph that operates from 0.9 to 2.4 microns. It will be deployed at the f/5 foci of the MMT and Magellan 6.5m telescopes. Using a fully refractive design, MMIRS offers R=1200-3000 spectral resolution with a spatial resolution of 0.2 arcsec per pixel on a 2kx2k Hawaii-2 array. We describe the optics, optics mounts, wavefront sensors, and wavelength calibration systems.

**Keywords:** spectrographs, infrared, imaging

## 1. INTRODUCTION

MMIRS is a slitmask based cryogenic imaging spectrograph that will be deployed at the f/5 focus of the converted MMT and the Magellan Clay telescopes. The design of MMIRS is based on that of the FLAMINGOS and FLAMINGOS2<sup>1-3</sup> instruments built at the University of Florida. In this paper we highlight several of the design features of MMIRS that have not been described previously.<sup>4</sup> The detector electronics for MMIRS were first developed for the Smithsonian Widefield Infrared Camera.<sup>5</sup>

## 2. OPTICAL DESIGN

### 2.1. Overview

The optical design for MMIRS is comprised of three sections, a corrector, a collimator, and a camera. A layout of the optics is shown in Figure 1. The optics, including AR coatings, were all fabricated by Janos Technologies, in Keene, NH.

The two element CaF<sub>2</sub> corrector lies in front of the f/5 Cassegrain focus of the converted 6.5m MMT or Clay Magellan Telescope and produces images with RMS spot diameter less than 0''.1 over a 14' field of view. The first element of the corrector also serves as the vacuum window of the cryostat. With a thickness of 50mm it has a stress of 125 PSI from atmospheric pressure. The second corrector element is inside the cryostat but cools only slightly by radiation to the cold mechanisms below. It acts as a radiation shield to the first element, reducing its radiative cooling and any tendency to condense water on the outside.

Below the second corrector element lie pickoff mirrors for the guider assemblies (see section 2.3 below), a Dekker wheel to select the aperture size, and the slit wheel. The slit wheel contains a square imaging aperture, 7 long slits, varying in size from 0''.2 (1 pixel) to 2''(10 pixels), and 9 multislit masks, each 4'×7'. The pickoff mirror assembly is machined out of Aluminum-6061, diamond-turned, and then post-polished.

Separating the slit mask wheel from the collimator is a gate valve to isolate the optics and detector during slitmask changeout. The gate valve was manufactured by VAT of Switzerland. It is a slightly customized version of a catalog item. The valve is thin enough to allow a 100mm spacing between the slit and first collimator element as required by the optical design.

The 520mm focal length collimator has 6 elements, made of CaF<sub>2</sub>, CaF<sub>2</sub>, BaF<sub>2</sub>, ZnSe, Infrasil, and CaF<sub>2</sub>. It produces a 100mm diameter collimated beam. The filters are located just before the Lyot stop. We currently have four broadband filters, Y, J, H, and Ks, which are 125mm in dia and 10mm thick. They were purchased from Research Electro-Optic.

---

Further author information: Send correspondence to BAM E-mail: bmcleod@cfa.harvard.edu

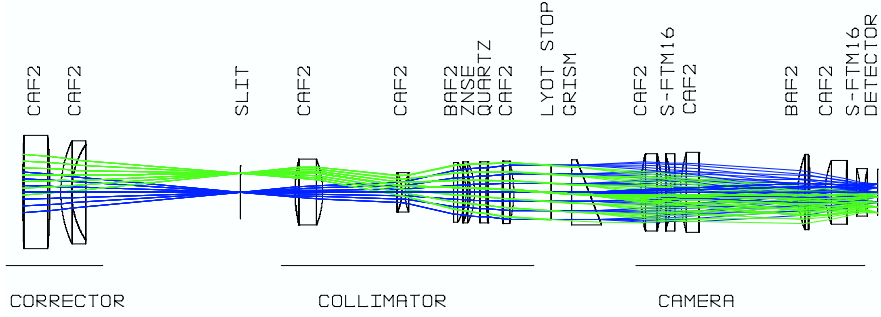


**Figure 1.** MMIRS Optics Layout

The Lyot stop was laser cut from 0.2mm thick anodized aluminum foil by PhotoMachining of Pelham, NH. The 33mm diameter central obscuration in the stop is supported by 0.75mm wide spider arms. These were made as thin as possible to minimize the amount of blocked light. Because the stop in the instrument is fixed, the Lyot stop spider will not line up with the telescope spider. After the Lyot stop is the wheel for the grisms which are discussed further in Section 2.2. The 280mm focal length camera optics also contains 6 elements, made of CaF<sub>2</sub>, S-FTM16, CaF<sub>2</sub>, BaF<sub>2</sub>, CaF<sub>2</sub>, and S-FTM16.

Figure 2 shows the final image quality expected from the as-built and assembled optics. The polychromatic spots are < 20 $\mu$ m RMS diameter, or just over 1 pixel, over the full 7' square field of view. The final scale is 0''.2 per pixel. We recently checked our design against recent refractive index measurements made by the CHARMS group at Goddard Space Flight Center.<sup>6,7</sup> We found that we did not need to make any changes other than a simple refocus. Indeed, initial cold tests of the optics have confirmed that we achieve the expected performance.

During the optical design process several constraints were introduced into the ZEMAX optimization operands to control ghost images. As a result, a ghost analysis shows that there are no significant ghost images or ghost pupils in the MMIRS optics.

## 2.2. Grisms

The instrument will initially have two grisms identical to those in Flamingos 2. The first grism will be a standard epoxy based replica grating mounted on an Infrasil prism and will provide R=1200 over the H and K bands. A second transmission grating on an Infrasil disk will be paired with a ZnSe prism to provide R=3000 in J, H, or K using higher orders.

## 2.3. Guiding and Wavefront Sensing

A pair of pickoff mirrors just above the focal plane will direct light into two identical guider/wavefront sensor assemblies. The guiding area is located outside of the 7'  $\times$  7' area out to a maximum radius of 7'. Each guider

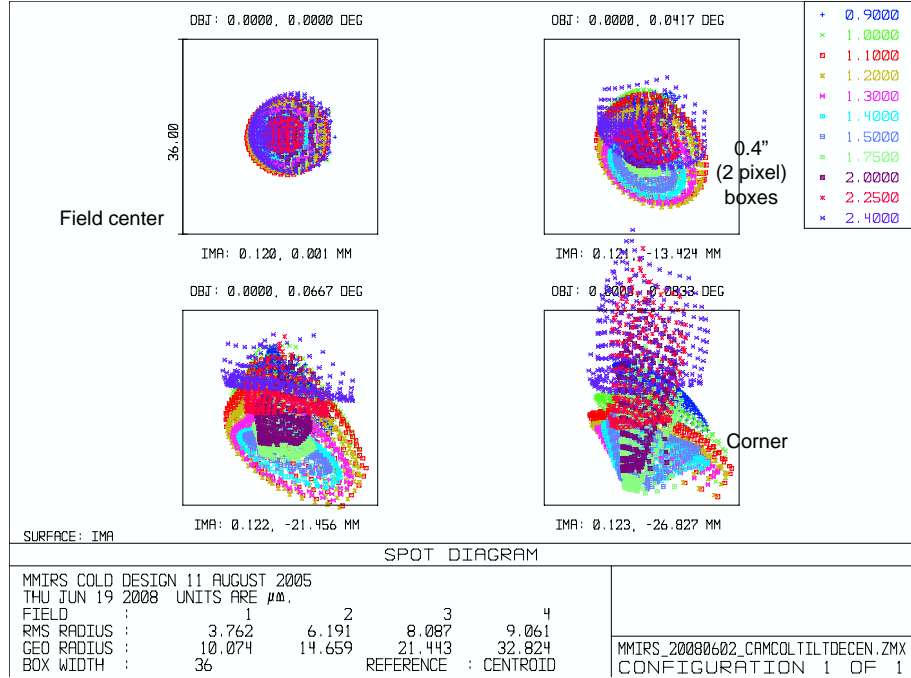


**Figure 2.** Spot diagrams for MMIRS using as built radii, thicknesses, and measured decenter and tilt assembly errors, polychromatic from 0.9-2.4 $\mu\text{m}$ . The box is 0''.4 square.

assembly is located outside the vacuum on a 3-axis stage (x, y, and focus). The focal plane is relayed 1:1 onto the guider camera with an f/2.8 150mm Sigma EX DG commercial macro lens. The field of view of each guide camera is 1.3 $\times$ 1.3. For wavefront sensing, fold mirrors can be inserted into the beam which direct the light through a Shack-Hartmann wavefront sensor. The wavefront sensor contains an aperture to limit the field of view to minimize sky background, a collimating lens, and the lenslet array. An LED illuminated pinhole located inside the cryostat provides a calibration source for the wavefront sensor. We expect to use one camera in guide mode and the other in wavefront sensing mode.

## 2.4. Calibration Lamps

Our calibration lamps will be provided by a simple compact system that provides a proper f/5 beam into the instrument. We use a LabSphere 6 inch integrating sphere with their IR coating. The 2.5 inch exit port of the sphere is conjugated to the Lyot stop using an IR transmissive Fresnel lens. The system evenly illuminates the full 7x7 arcmin field. The two one-inch ports on the sphere will contain continuum lamps and He-Ne-Ar Penray line lamps. A fold mirror translates in front of the instrument to view the calibration system.

## 3. MECHANICAL DESIGN

### 3.1. Layout

The layout of the instrument is shown in Figure 3. The top section of the instrument is the MOS chamber. The toroidal LN<sub>2</sub> reservoir is supported by an insulating G-10 ring from the bulkhead separating the two cryostat sections. The top of the MOS LN<sub>2</sub> reservoir serves as the mounting plate for the MOS and Dekker wheels and the guider pickoff mirrors. To the sides are two windows that send the guider light outside the cryostat. Below the MOS mechanisms is the gate valve, and immediately below this is the first collimator element.

Mounted from the bottom of the bulkhead is a second G-10 ring which supports a D-shaped LN2 reservoir in the camera section. The face of this reservoir is the bench to which all the optics are mounted.

### 3.2. Optics mounts

The MMIRS cryogenic optics mount design (Figure 4) uses aspects of the optics mounts that are used in the Gemini Near Infrared Spectrograph (GNIRS)<sup>8</sup> and EMIR.<sup>9</sup> The lenses are mounted in Aluminum housings. Radially they are constrained by two Delrin pads 40 degrees in angular extent. The angular size of the pads were chosen to minimize the compressive stress put on the lens. The thickness of the pads is chosen so that the lenses are centered at room temperature and also at 77K. All the Delrin parts were made from the same batch of material, of which we had the CTE measured. The radial spring forces are provided by compression springs selected from the Lee Spring catalog.

Our tolerance analysis indicated that we could tolerate radial positioning errors of each lens distributed uniformly within a 75 microns radius circle. A downside of the pads being 40 degrees in angular extent is that a small error in the thickness of the pad produces a displacement of the lens approximately ( $1/\sin(10^\circ) \approx 6$ ) times larger than the error in the pad thickness. Even so, radial error distribution met our error budget with some room to spare.

Axially each lens is constrained by three raised Aluminum pads each 40 deg long and 5mm wide. Between the pad and the lens is a 0.003" thick Kapton spacer. The opposite side of the lens provides the axial spring force via a Teflon spacer, an aluminum spacer with three more matching raised pads, a custom made beryllium copper Belleville spring and an aluminum spring retainer. The springs were designed to provide a 10G force.

The lens mount parts were manufactured to the tolerance required to meet the optical alignment specification without need for shimming or adjustment. In practice, the process of verifying that the parts were made correctly, developing the procedure to safely insert each lens into its housing, and verifying that each lens ended up in the correct place required approximately one week per lens. The first step was mechanical measurement of the critical dimensions, either with digital calipers or with a computerized measuring machine (CMM). Then each part was cleaned and inspected for small burrs under a microscope.

After the lens was installed we measured its decenter, tilt, and axial placement relative to its housing using a TriOptics Opticentric machine. The Opticentric consists of a rotary table on an air bearing. The table has tip-tilt and X-Y translation manual control. Located on either side of the table is an autocollimator equipped with a video camera. Using an appropriate head lens on each autocollimator focused at the center of curvature of the lens surface we see the autocollimator cross hairs in focus on the camera. We then adjust the tilt and translation of the table to bring the lens optical axis onto the rotary axis of the air bearing. The final step is to measure the mechanical runout of the lens housing using a digital indicator. We can also measure the axial position of the lens by focusing the autocollimator head lens onto the surface of the lens. Our measurement repeatability with the Opticentric is less than 10 microns of decenter, 0.1 mrad of tilt, and 25 microns axially.

### 3.3. Mechanisms

The original design of MMIRS had the slitmask, dekker, filter and grism wheels, and focus stage each cooled via sapphire ball bearings. Although formal calculations indicated that this would provide ample cooling, in practice this was not borne out. This shortcoming is believed to be because of the point contacts between the balls and the bearing grooves. Because the focus stage has a linear motion of only a few mm, adding copper straps was sufficient to solve the cooling problem there. The grism and filter wheels are enclosed in a box and do not require particularly fast cooldown and warmup, so radiative cooling is sufficient to cool them. The MOS and Dekker wheels pose more of a challenge. They are required to cool to within 10K of their final temperature within a two hour period, and warm up similarly fast. We are currently investigating the use of ESLI's Veltherm product. This carbon fiber velvet has high thermal conductivity and fills the space between the shaft (now made of Be Copper) and the wheel body. Teflon shaft seals located above and below the Veltherm trap any fibers that may come loose from the velvet.

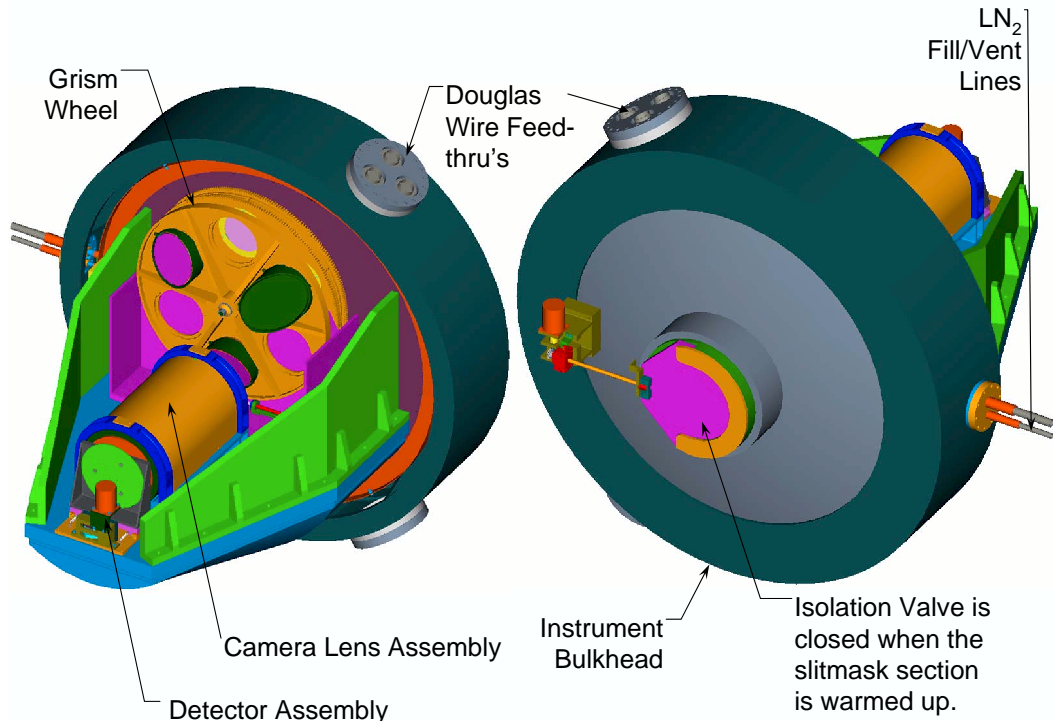
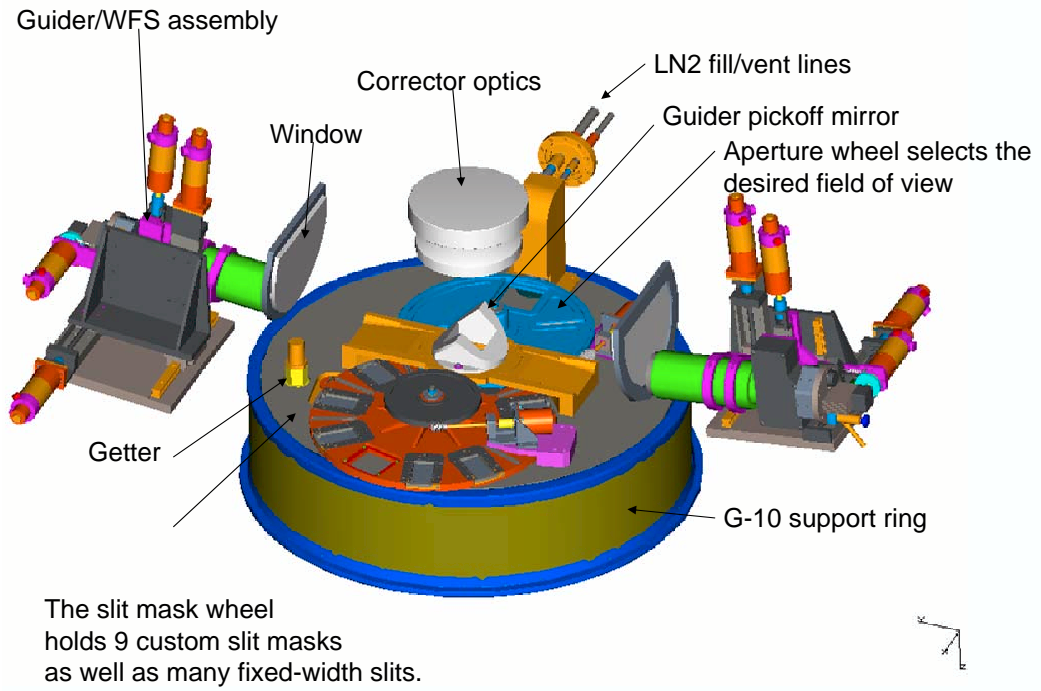


**Figure 3.** Layout of MMIRS. The distance from the top of the corrector to the detector is 1.6m.

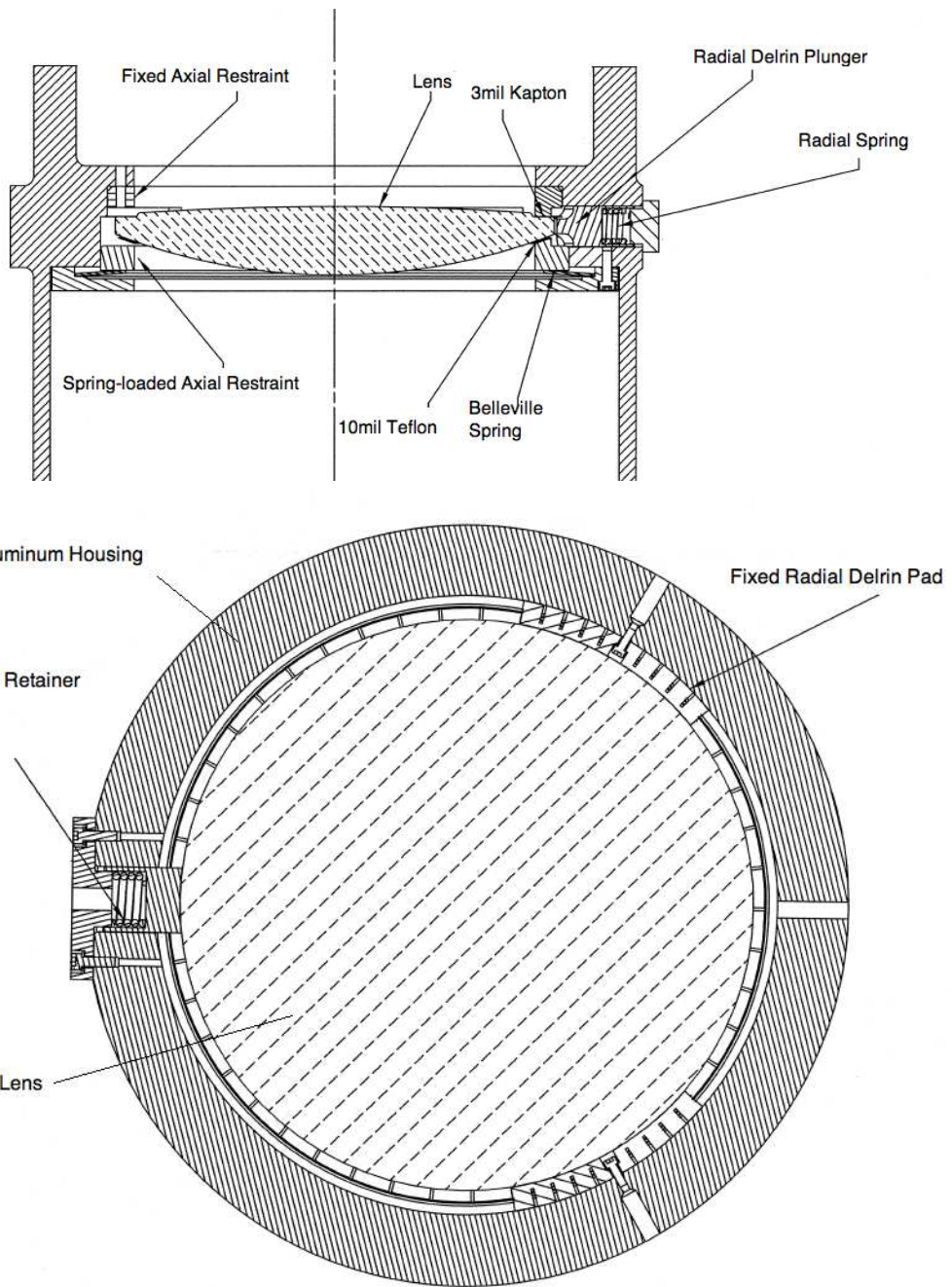


Figure 4. Radial and axial section views of a typical lens mount.

## 4. ELECTRICAL DESIGN

### 4.1. Motion Control

The mechanisms are all powered by Phytron cryogenic stepper motors and driven by Phytron stepper motor drivers under control of a DeltaTau CMAC motion controller. Each wheel has a pair of redundant in-position switches on the detent mechanism.

### 4.2. Vacuum and interlock system

MMIRS includes a turbo pump mounted directly to the MOS dewar. This pump will be used during slit mask changeouts and also for the less frequent pumpouts of the main dewar. A vacuum interlock system implemented in hardware monitors the pressure and temperature on both sides of the gate valve. The interlock system prevents the gate valve from being opened when the MOS dewar is at atmospheric pressure. It also locks out the back fill valves so the MOS section cannot be raised to ambient pressure if the gatevalve is open and the optics section is cold. Finally, the interlock prevents the MOS heaters from being turned on when the gate valve is open.

### 4.3. Controlled cooldown

The cooldown and warmup of the optics section of MMIRS is controlled to minimize stress on the optics and detector. The control is accomplished with a Valcor cryogenic valve, an Omega temperature controller, and an RTD mounted on the curved back surface of the dewar at the end under the detector. The setpoint is ramped downwards at 0.15K/min through software. A threshold prevents the setpoint from dropping more than 5K below the actual temperature. This is a safety feature so that if the flow of cryogen is temporarily interrupted and then restored (e.g. when swapping from an empty LN2 tank to a full one) , there will not be a sudden drop in temperature. A 1/16 inch orifice at the end of the LN2 fill line prevents the maximum flow rate of LN2 from exceeding more than about a factor of two above the nominal flow rate. This guards against rapid cooling in the unlikely event of the valve sticking open.

The warmup is controlled in a similar manner. Cartridge heaters soldered into a copper block are bolted to the top of the optical bench. Additional heaters are mounted onto the detector board. The detector board heaters, driven by a Lakeshore controller, are used to stabilize the temperature during normal operation. During warmup the optical bench heater setpoint is set a few degrees below that of the detector board to minimize freezing outgassed material onto the detector. Again threshholds prevent the setpoints from deviating from the actual temperatures so that loss of power will not cause a sudden drop in temperature.

Thermostats mounted on the heater blocks prevent current from going through the heater when the temperature rises above 40C. This guards against catastrophic heating in the event of a control system failure.

## ACKNOWLEDGMENTS

This material is based upon work supported by AURA through the National Science Foundation under Scientific Program Order No. 5 as issued for support of the Telescope Systems Instrumentation Program (TSIP), in accordance with Proposal No. AST-0335461 submitted by AURA.

We thank S. Eikenberry, N. Raines, and J. Julian at the University of Florida for their support in adapting the Flamingos-2 design to MMIRS.

## REFERENCES

1. R. Elston, “FLAMINGOS: a multiobject near-IR spectrometer,” in *Proc. SPIE Vol. 3354, p. 404-413, Infrared Astronomical Instrumentation, Albert M. Fowler; Ed.,* pp. 404–413, Aug. 1998.
2. R. Elston, S. N. Raines, K. T. Hanna, D. B. Hon, J. Julian, M. Horrobin, C. F. W. Harmer, and H. W. Epps, “Performance of the FLAMINGOS near-IR multi-object spectrometer and imager and plans for FLAMINGOS-2: a fully cryogenic near-IR MOS for Gemini South,” in *Instrument Design and Performance for Optical/Infrared Ground-based Telescopes. Edited by Iye, Masanori; Moorwood, Alan F. M. Proceedings of the SPIE, Volume 4841, pp. 1611-1624 (2003).,* pp. 1611–1624, Mar. 2003.

3. S. Eikenberry, R. Elston, S. N. Raines, J. Julian, K. Hanna, D. Hon, R. Julian, R. Bandyopadhyay, J. G. Bennett, A. Bessoff, M. Branch, R. Corley, J.-D. Eriksen, S. Frommeyer, A. Gonzalez, M. Herlevich, A. Marin-Franch, J. Marti, C. Murphey, D. Rashkin, C. Warner, B. Leckie, W. R. Gardhouse, M. Fletcher, J. Dunn, R. Wooff, and T. Hardy, "FLAMINGOS-2: the facility near-infrared wide-field imager and multi-object spectrograph for Gemini," in *Ground-based and Airborne Instrumentation for Astronomy. Edited by McLean, Ian S.; Iye, Masanori. Proceedings of the SPIE, Volume 6269*, pp. 626917 (2006)., Presented at the Society of Photo-Optical Instrumentation Engineers (SPIE) Conference **6269**, July 2006.
4. B. A. McLeod, D. Fabricant, J. Geary, P. Martini, G. Nystrom, R. Elston, S. S. Eikenberry, and H. Epps, "MMT and Magellan infrared spectrograph," in *Ground-based Instrumentation for Astronomy. Edited by Alan F. M. Moorwood and Iye Masanori. Proceedings of the SPIE, Volume 5492*, pp. 1306-1313 (2004)., A. F. M. Moorwood and M. Iye, eds., Presented at the Society of Photo-Optical Instrumentation Engineers (SPIE) Conference **5492**, pp. 1306–1313, Sept. 2004.
5. W. R. Brown, B. A. McLeod, J. C. Geary, and B. E. C., "Smithsonian Widefield Infrared Camera," in *Ground-based and Airborne Instrumentation for Astronomy. Proceedings of the SPIE, Volume 7014*, pp. xxx-xxx (2008)., Presented at the Society of Photo-Optical Instrumentation Engineers (SPIE) Conference, pp. 7014–xxx, 2008.
6. D. B. Leviton, B. J. Frey, and T. Kvamme, "High accuracy, absolute, cryogenic refractive index measurements of infrared lens materials for JWST NIRCam using CHARMS," in *Cryogenic Optical Systems and Instruments XI. Edited by Heaney, James B.; Burriesci, Lawrence G. Proceedings of the SPIE, Volume 5904*, pp. 222-233 (2005)., J. B. Heaney and L. G. Burriesci, eds., Presented at the Society of Photo-Optical Instrumentation Engineers (SPIE) Conference **5904**, pp. 222–233, Aug. 2005.
7. D. B. Leviton, B. J. Frey, and T. J. Madison, "Temperature-dependent refractive index of CaF<sub>2</sub> and Infrasil 301," in *Cryogenic Optical Systems and Instruments XII. Edited by Heaney, James B.; Burriesci, Lawrence G.. Proceedings of the SPIE, Volume 6692*, pp. 669204 (2007)., Presented at the Society of Photo-Optical Instrumentation Engineers (SPIE) Conference **6692**, Oct. 2007.
8. "Prototype Lens Mount Tests," Tech. Rep. GNIRS SDN21.05, NOAO, 2003.
9. S. Barrera, A. Villegas, J. Fuentes, S. Correa, J. Pérez, P. Redondo, R. Restrepo, V. Sánchez, F. Tenegi, F. Garzón, and J. Patrón, "EMIR optomechanics," in *Astronomical Structures and Mechanisms Technology. Edited by Antebi, Joseph; Lemke, Dietrich. Proceedings of the SPIE, Volume 5495*, pp. 611-621 (2004)., J. Antebi and D. Lemke, eds., Presented at the Society of Photo-Optical Instrumentation Engineers (SPIE) Conference **5495**, pp. 611–621, Sept. 2004.